



Published in final edited form as:

*J Immunol.* 2009 November 15; 183(10): 6296–6302. doi:10.4049/jimmunol.0900613.

## Localization of Kv1.3 channels in the immunological synapse modulates the calcium response to antigen stimulation in T lymphocytes<sup>1</sup>

Stella A. Nicolaou<sup>\*,‡</sup>, Lisa Neumeier<sup>\*,‡</sup>, Ashleigh Steckly<sup>\*</sup>, Vladimir Kucher<sup>\*</sup>, Koichi Takimoto<sup>§</sup>, and Laura Conforti<sup>\*,‡</sup>

<sup>\*</sup>Department of Internal Medicine, University of Cincinnati, Cincinnati, OH, 45267, USA

<sup>‡</sup>Department of Molecular and Cellular Physiology, University of Cincinnati, Cincinnati, OH, 45267, USA

<sup>§</sup>Department of Bioengineering, Nagaoka University of Technology, Nagaoka, Niigata 940-2188, Japan

### Abstract

The immunological synapse (IS), a highly organized structure that forms at the point of contact between a T cell and an antigen presenting cell, is essential for the proper development of signaling events including the Ca<sup>2+</sup> response. Kv1.3 channels control Ca<sup>2+</sup> homeostasis in human T cells and move into the IS upon antigen presentation. However, the process involved in channel accumulation in the IS and the functional implications of this localization are not yet known. Here we define the movement of Kv1.3 into the IS and study whether Kv1.3 localization into the IS influences Ca<sup>2+</sup> signaling in Jurkat T cells. Crosslinking of the channel protein with an extracellular antibody limits Kv1.3 mobility and accumulation at the IS. Moreover, Kv1.3 recruitment to the IS does not involve the transport of newly synthesized channels and it does not occur through recycling of membrane channels. Kv1.3 localization in the IS modulates the Ca<sup>2+</sup> response. Blockade of Kv1.3 movement into the IS by crosslinking significantly increases the amplitude of the Ca<sup>2+</sup> response triggered by anti-CD3/anti-CD28 coated beads which induce the formation of the IS. On the contrary, the Ca<sup>2+</sup> response induced by TCR stimulation without the formation of the IS with soluble anti-CD3/anti-CD28 antibodies is unaltered. The results presented herein indicate that, upon antigen presentation, membrane-incorporated Kv1.3 channels move along the plasma membrane to localize in the IS. This localization is important to control the amplitude of the Ca<sup>2+</sup> response and disruption of this process can account for alterations of downstream Ca<sup>2+</sup>-dependent signaling events.

<sup>1</sup>This work was supported by NIH grants #CA95286, #AI083076 and AHA Ohio Affiliate Grant-in-aid #0855457D to LC. SAN was supported by a AHA Ohio Affiliate Fellowship #0615213B and AS by a fellowship of the NSF-REU program #0647677.

Send correspondence to: Laura Conforti, Department of Internal Medicine, 231 Albert Sabin Way, University of Cincinnati, Cincinnati, OH 45267-0585, Phone # (513) 558-6009, Fax # (513) 558-4309, Laura.Conforti@uc.edu.

<sup>‡</sup>SAN and LN contributed equally to this work.

**Publisher's Disclaimer:** "This is an author-produced version of a manuscript accepted for publication in *The Journal of Immunology* (*The JI*). The American Association of Immunologists, Inc. (AAI), publisher of *The JI*, holds the copyright to this manuscript. This version of the manuscript has not yet been copyedited or subjected to editorial proofreading by *The JI*; hence, it may differ from the final version published in *The JI* (online and in print). AAI (*The JI*) is not liable for errors or omissions in this author-produced version of the manuscript or in any version derived from it by the U.S. National Institutes of Health or any other third party. The final, citable version of record can be found at [www.jimmunol.org](http://www.jimmunol.org)."

## Keywords

Calcium; T cell activation; ion channels

---

## INTRODUCTION

Ion channels are important modulators of T cell function as they regulate the membrane potential and  $\text{Ca}^{2+}$  influx during T cell activation. T cell activation is initiated by the presentation of the antigen to the T cells through antigen presenting cells (APC) such as B lymphocytes and dendritic cells. The initial recognition phase is followed by a cascade of signaling events. An increase in intracellular  $\text{Ca}^{2+}$  concentration ( $[\text{Ca}^{2+}]_i$ ) occurs very early upon T cell activation and this increase is essential for cytokine release and proliferation (1). Indeed  $\text{Ca}^{2+}$  is a key regulator of the activity of important transcription factors in T lymphocytes (1,2). The increase in  $[\text{Ca}^{2+}]_i$  upon T cell activation depends on various membrane channels and transporters.

The main ion channels expressed in human T lymphocytes are the voltage-dependent Kv1.3 channel, the  $\text{Ca}^{2+}$ -sensitive KCa3.1 channel and the  $\text{Ca}^{2+}$ -release activated  $\text{Ca}^{2+}$  channel (CRAC) (3,4). These channels act in concert to regulate the onset and development of the  $\text{Ca}^{2+}$  response upon encounter with an antigen. The sequence of events triggered upon activation of the T cell receptor (TCR) can be summarized as follows: TCR stimulation induces the release of  $\text{Ca}^{2+}$  from the endoplasmic reticulum (ER) via phospholipase C  $\gamma$  (PLC- $\gamma$ ) activation and production of inositol-3-phosphate (IP3). Once ER  $\text{Ca}^{2+}$  stores are sufficiently depleted, stromal interaction molecule 1 (STIM1) in the ER moves into proximity to, and activates, Orai1 (a pore-forming subunit of the CRAC channel) and  $\text{Ca}^{2+}$  influx begins (4,5). The activity of CRAC channels is facilitated by membrane hyperpolarization which increases the total driving force for  $\text{Ca}^{2+}$  entry. Kv1.3 and KCa3.1 channels regulate membrane potential. Thus, opening of Kv1.3 and KCa3.1 channels enhances  $\text{Ca}^{2+}$  entry by hyperpolarizing the cell membrane, while their inhibition suppresses the  $\text{Ca}^{2+}$  response (6,7). Along with allowing initiation of the  $\text{Ca}^{2+}$  influx, the crosstalk between these and other channels/transporters determines the amplitude and duration of the  $\text{Ca}^{2+}$  response (1).

Recent evidence indicates that Kv1.3, KCa3.1 and CRAC channels are redistributed in the immunological synapse (IS) (8-11). The IS is a tight and highly organized interactive signaling zone localized at the point of contact between T cell and APC, containing membrane proteins (e.g., TCR, CD3 and LFA-1) and signaling molecules (12,13). The structure of the IS is dynamic and different configurations are achieved with time. Initially, small TCR clusters form and the activation response begins. Eventually, these clusters organize into a mature structure characterized by its "bull's eye" configuration with a central TCR cluster (cSMAC) and a peripheral adhesion molecule ring (pSMAC) (12,14). Functionally, IS formation is thought to fine-tune the outcome of TCR engagement. It has been shown that the mature synapse functions as a signal terminator by facilitating TCR degradation and reducing the  $\text{Ca}^{2+}$  response (15, 16). Mossman et al. have shown that disruption of the formation of a mature synapse is associated with an increased  $\text{Ca}^{2+}$  response (15). Quintana et al. showed that the redistribution of mitochondria to the IS upon TCR activation guarantees  $\text{Ca}^{2+}$  uptake at this site and maintenance of  $\text{Ca}^{2+}$  influx (17). We have also shown that Kv1.3 channels are rapidly recruited to the IS upon T cell activation and herein persist for a long time (9). Furthermore, this process is altered in T cells from patients with the autoimmune disease Systemic Lupus Erythematosus (SLE) (9). Since SLE T cells display abnormalities in the  $\text{Ca}^{2+}$  response to TCR stimulation, Kv1.3 trafficking to the IS may be essential for the proper  $\text{Ca}^{2+}$  signaling (9,18).

These findings suggest the importance of localization and regionalized function of Kv1.3 channels in the IS. Yet, the mechanisms mediating the channel localization to the IS and the functional significance of this rearrangement are not understood. Herein we performed studies to elucidate the movement of Kv1.3 channels to the IS and its functional consequence on Ca<sup>2+</sup> signaling.

## MATERIALS AND METHODS

### Cells

Jurkat T cells (American Tissue Culture Collection, Masassas, VA) were maintained in RPMI medium supplemented with 10% fetal bovine serum (FBS) (Fisher Scientific, Pittsburgh, PA), 100 U/ml penicillin, 100 µg/ml streptomycin and 1 mM Hepes as previously described (19).

### Crosslinking

Surface Kv1.3 proteins were immobilized by antibody complexes with rabbit anti-Kv1.3 antibody and secondary anti-rabbit antibody. Briefly, Jurkat cells were incubated on ice for one hour with polyclonal anti-Kv1.3 antibody against an extracellular epitope (EC-Kv1.3, Sigma-Aldrich cat # P4497, St. Louis, MO) at 100:1 ratio of antibody:Kv1.3  $\alpha$  subunit (0.8 µg antibody/10 ml cell suspension of 2 million cells/ml), unless otherwise indicated. This concentration was determined considering, on average, the expression of ca. 400 Kv1.3 channels/cell and the fact that each channel is formed by four  $\alpha$  subunits. The incubation with Kv1.3 antibody was followed by a 30-minute incubation with anti-rabbit IgG. Control cells underwent the same experimental steps with either isotype IgG or without antibody, as specified in the text.

### Measurement of Intracellular Calcium

Jurkat cells were loaded with 1 µM Fura-2/AM and the experiments were performed on a Cyt-Im2 Ca<sup>2+</sup> imaging system (Intracellular Imaging, Cincinnati, OH) as previously described (20). Experiments were performed at 34.3 ± 0.2°C (n=29). Fura-2 loaded cells were recorded while bathed in 0.5 mM Ca<sup>2+</sup> Ringer solution for 2 min before addition of either anti-CD3/CD28 coated beads (Invitrogen) or soluble anti-CD3 antibody (OrthoBiotech Products) or a mixture of soluble anti-CD3 and anti-CD28 antibodies (BD Pharmingen). Visual inspection showed formation of stable bead/T cell conjugates in the bath. Absolute intracellular Ca<sup>2+</sup> concentrations ([Ca<sup>2+</sup>]<sub>i</sub>) were obtained using the formula: [Ca<sup>2+</sup>]<sub>i</sub> = Kd (R-R<sub>min</sub>)/(R<sub>max</sub>-R) \* F380min/F380max, where Kd= effective fura-2 dissociation constant, R= 340/380 ratio, R<sub>min</sub>= R at 0 Ca<sup>2+</sup>, R<sub>max</sub>= R of maximum saturating Ca<sup>2+</sup> and F380min/F380max is the ratio of the 380 nm intensity of Fura-2 at minimum and maximum saturating Ca<sup>2+</sup>. The Kd was empirically derived using human CD4<sup>+</sup> T cells and calibration buffers with estimated free [Ca<sup>2+</sup>]<sub>i</sub> of 0-30 µM (Molecular Probes, Inc., Eugene, OR). We measured a Kd of 250 ± 7 nM (n=2) at 34.7 ± 0.1 °C which is in agreement with previous reports (21). R<sub>min</sub> was measured after every experiment using 0 mM Ca<sup>2+</sup> Ringer solution in the presence of 3 µM ionomycin. R<sub>max</sub> was also measured after every experiment using 2.5 mM Ca<sup>2+</sup> Ringer solution. We observed no difference in R<sub>max</sub> when using 10 mM Ca<sup>2+</sup> Ringer solution. The Ca<sup>2+</sup> response is expressed as changes in [Ca<sup>2+</sup>]<sub>i</sub> ( $\Delta$ [Ca<sup>2+</sup>]<sub>i</sub>) elicited upon TCR stimulation and it was determined by subtracting the baseline [Ca<sup>2+</sup>]<sub>i</sub> from the peak and steady-state (5 min from onset of the Ca<sup>2+</sup> response) [Ca<sup>2+</sup>]<sub>i</sub>. To obtain the average [Ca<sup>2+</sup>]<sub>i</sub> response we included only cells that showed a significant increase of [Ca<sup>2+</sup>]<sub>i</sub> after stimulation and these cells were synchronized to reflect initiation of Ca<sup>2+</sup> influx as previously described (10). Briefly, we considered cells with a significant increase in Ca<sup>2+</sup> those cells that had an increase in 340/380 ratio ≥0.1 ratio units. We have previously established that this value is well above two standard deviations of the average background noise (10). We excluded cells that display [Ca<sup>2+</sup>]<sub>i</sub> oscillation before stimulation and did not respond to TCR engagement. Cells that did not

respond, but showed an increase in  $[Ca^{2+}]_i$  with ionomycin (1-2  $\mu$ M), added at the end of the experiment, were considered non-responding cells. To determine the distribution of  $Ca^{2+}$  responses we defined as transient responses brief  $[Ca^{2+}]_i$  increases that return to baseline within the 15 min duration of the experiment; sustained responses as  $Ca^{2+}$  responses that are followed by a sustained plateau that is maintained for the whole duration of the experiment; oscillatory as  $Ca^{2+}$  responses that include three or more peaks in  $[Ca^{2+}]_i$  during the 15 min recording. The number of cells displaying a specific response was reported as % of total responding cells. We also measure the frequency of oscillations as previously described (22). The data analysis was performed using the program Microcal Origin 5.0 (Microcal Software Inc., Northampton, MA) and Microsoft Office Excel with home-written macros. When beads were added in the bath they made contact with T cells at various time points. To allow for direct comparison, time points prior to 50 sec before the first oscillation were excluded. The data were fitted using a third order polynomial function. Next, the data were analyzed using the fast fourier transform (FFT) algorithm and the FFT data were then used to determine the power spectral density (PSD), which provides information regarding oscillation frequency. For each cell the frequency was determined by using the PSD maximum value.

### Electrophysiology

Kv1.3 currents were induced in whole-cell configuration by depolarizing voltage steps from -80 mV holding potential (HP) to +50 mV applied every 30 s, as previously described (19). The external solution had the following composition (in mM): 150 NaCl, 5 KCl, 2.5  $CaCl_2$ , 1.0  $MgCl_2$ , 10 glucose and 10 HEPES, pH 7.4. The pipette solution was composed of (mM): 134 KCl, 1  $CaCl_2$ , 10 EGTA, 2  $MgCl_2$ , 5 ATP-sodium, and 10 HEPES, pH 7.4.

### T cell Activation and Immunocytochemistry

T cell activation with anti-CD3/CD28 coated beads (Invitrogen) and immunocytochemistry have been previously described (9). CD3 $\epsilon$  was visualized with anti-CD3 $\epsilon$  antibody (Santa Cruz Biotechnology, Inc., Santa Cruz, CA) and F-actin with Alexa Fluor 546 phalloidin (Invitrogen). Kv1.3 was visualized with either EC-Kv1.3 antibody or anti-Kv1.3 antibody against an intracellular epitope (Kv1.3 ab, Sigma, cat#P9107) as specified in the text or figure legends. Images were acquired using either a Nikon Microphot FXA or a Zeiss Axioplan Imaging 2 infinity-corrected upright scope coupled to an Orca-ER cooled camera (Axioscope, Carl Zeiss, Microimaging Inc.), Plan-Apochromat 60X-100X oil immersion objectives and the appropriate filters. Proteins' accumulation at the bead/T cell point of contact was analyzed as follows: boxes of equal area were drawn around the IS and in the area most representative of the membrane outside the IS (9). The mean fluorescence ratio (MFR) was then calculated as follows:  $MFR = [\text{Mean Fluorescence Intensity (MFI) at the IS-background}] / [\text{MFI outside the IS-background}]$ . Based on our previous experiments, T cell/bead conjugates that displayed a  $MFR \geq 1.5$  were scored positive for protein polarization in the IS (9). The data were analyzed using the Metamorph computer software with home-written macros.

### Statistical Analysis

All data are presented as means  $\pm$  SEM. Statistical analyses were performed using Student's t-test (paired or unpaired);  $p \leq 0.05$  was defined as significant. The Wilcoxon Signed Rank Test was used for non-normal distribution and/or unequal variances.

## RESULTS

### Redistribution of Kv1.3 channels in the IS occurs by lateral movement along the plasma membrane

We tested whether native Kv1.3 channels accumulate in the IS by lateral movement along the plasma membrane. We hypothesized that, if indeed this was the case, crosslinking of surface Kv1.3 channels should prevent their recruitment to the IS. We took advantage of the availability of an antibody against an extracellular epitope located in the loop between the membrane spanning domains S1 and S2 of the Kv1.3 polypeptide, far from the conducting pore (EC-Kv1.3 antibody) (23). Live Jurkat cells were incubated with EC-Kv1.3 antibody followed by secondary antibody to crosslink the surface channel proteins. This intervention was designed to entrap the Kv1.3 membrane proteins in an antibody network that limits the channel mobility upon encounter with an APC. This antibody is specific for Kv1.3 as pre-adsorption to the antigen peptide eliminates the fluorescent signal (Fig. 1A) (9). More importantly, the binding of this antibody to the channel protein and subsequent application of secondary anti-rabbit antibody did not alter Kv1.3 activity (Fig. 1B-D). Kv1.3 crosslinking results in the formation of clusters/puncta of Kv1.3 proteins in the membrane, but other proteins that are recruited at the IS such as CD3 $\epsilon$  remain uniformly distributed (Fig. 2A). The crosslinked cells were then exposed to CD3/CD28 beads and the degree of Kv1.3 accumulation in the IS determined. Microscopy experiments showed that Kv1.3 crosslinking prevents the translocation of channel proteins to the IS (Fig. 2B and D). No inhibition of Kv1.3 recruitment into the IS was observed with isotype IgG instead of anti-Kv1.3 antibody. The Kv1.3 recruitment in the IS with rabbit IgG was  $54.7 \pm 5.4$  (SD)% (n=2 experiments, on average 64 conjugates/experiment). Kv1.3 crosslinking did not affect the formation of the IS, as F-actin and CD3 $\epsilon$  accumulation to the bead/T cell contact site were preserved (Fig. 2B-D). Overall, the crosslinking of membrane-incorporated Kv1.3 channels reduced the accumulation of channel proteins in the IS by  $90 \pm 5\%$  (Fig. 2D).

### Kv1.3 recruitment to the IS does not involve the transport of newly synthesized channels and it does not occur through recycling of membrane channels

To test if Kv1.3 recruitment involves the transport of newly synthesized channels, further experiments were conducted in the presence of the protein synthesis inhibitor cycloheximide (CHX) (Fig. 3A) (24). Jurkat cells were pre-treated overnight with CHX (10  $\mu$ M) and then exposed to CD3/CD28 beads. The degree of Kv1.3 polarization in the IS was then determined in these cells by fluorescent microscopy and compared to untreated cells. CHX treatment, which deprives cells of newly synthesized proteins, did not affect the extent of Kv1.3 recruitment in the IS indicating that the accumulation of Kv1.3 in the IS reflects the movement of mature channel proteins present at the plasma membrane. Overall these data support the hypothesis that the recruitment of Kv1.3 at the IS results from the lateral movement of membrane-incorporated channels. Further experiments were conducted to determine whether Kv1.3 localization into the IS occurs by endocytosis of membrane incorporated channels and their subsequent re-insertion in the plasma membrane at the IS. It has been shown that Kv channels can undergo the rapid recycling shuffle between endosomes and the cell surface (25). We studied if inhibition of either endocytosis or exocytosis by dynamin inhibitor peptide (DIP) and low temperature (20°C), respectively, prevented Kv1.3 translocation to the IS (Fig. 3B). DIP blocks dynamin, which is responsible for the clipping of nascent endocytotic vesicles from the membrane, while a 20°C temperature is sufficient to allow normal internalization of endocytotic vesicles, but it is not compatible with recycling to the plasma membrane (26). Specifically, we exposed Jurkat T cells to either DIP (50  $\mu$ M) or equal concentrations of DIP scramble control overnight and after that we measured the degree of Kv1.3 localization into the IS and compared. For the exocytosis experiments, we compared the degree of Kv1.3 polarization in T cells at 20°C to that of cells maintained at 37°C. These same experimental

conditions were used to study how retrograde trafficking regulates surface expression of Kv1.5 (26). We observed that neither intervention inhibits Kv1.3 localization indicating that Kv1.3 recruitment into the IS occurs by lateral movement in the plane of the membrane.

### Blockade of Kv1.3 trafficking to the IS alters the Ca<sup>2+</sup> response to antigen stimulation

The functional implications of Kv1.3 localization in the IS are still not known. It has been speculated that the recruitment of ion channels in this signalosome may be important to regulate Ca<sup>2+</sup> signaling (9,11,27). A direct way to prove this is to prevent the channel trafficking to the IS and determine if this intervention alters TCR-mediated Ca<sup>2+</sup> response. The previous section established that Kv1.3 crosslinking can be used to “mechanically” disrupt the movement of Kv1.3 to the IS, thus providing a simple and convenient experimental tool for trapping Kv1.3 outside the synapse. We used this approach to study the functional consequences of Kv1.3 trafficking to the IS.

Fura-2 experiments were performed to measure the Ca<sup>2+</sup> response to antigen stimulation in Kv1.3 crosslinked (XL) and untreated (CTR) Jurkat cells (Fig. 4). Antigen stimulation was produced by exposure to CD3/CD28 beads as surrogate APCs (9). A large fraction of XL and CTR cells responded to antigen presentation with an increase in [Ca<sup>2+</sup>]<sub>i</sub>. The percentages of responding cells were 74±7% in CTR and 84±4% in XL (n=8; p=0.1). The CD3/CD28 beads elicited a variety of Ca<sup>2+</sup> responses (Fig. 4A). However, the average Ca<sup>2+</sup> response triggered by beads differed between CTR and XL responding cells. We found that crosslinking and blockade of Kv1.3 translocation to the IS significantly increased the peak [Ca<sup>2+</sup>]<sub>i</sub> by 1.8±0.2 folds (n=8, p=0.002) (Fig. 4B top and D). This effect was not associated with a change in the rate of Ca<sup>2+</sup> rise. We have fitted the Ca<sup>2+</sup> rise with a Boltzmann equation and compared the time at 50% [Ca<sup>2+</sup>]<sub>i</sub> (t<sub>1/2</sub>) and the slope in control and crosslinked cells. The t<sub>1/2</sub> were 199.1 ±12.3 s in CTR and 192.3±11.1 s in XL (n=8; p=0.228). The slopes in CTR and XL were 11.7 ±1.8 and 13.1±1.5 nM/s, respectively (n=8; p=0.348). We also observed that in all but one experiment crosslinking on average increased steady-state [Ca<sup>2+</sup>]<sub>i</sub> by 1.7 ±0.3 folds (n=7; p=0.018) (Fig. 4B, bottom). On the contrary, the Ca<sup>2+</sup> response induced by TCR stimulation without the formation of the IS with either soluble anti-CD3 or anti-CD3/anti-CD28 antibodies was the same in CTR and XL cells (Fig. 4C-D). The average fold increase in [Ca<sup>2+</sup>]<sub>i</sub> by CD3/CD28 antibody in XL experiments was 1.0±0.1 folds (n=6, p=0.47, Fig. 4D), and that by CD3 antibody was 1.0±0.3 folds (n=5, p=0.70, Fig. 4D). No significant difference in baseline [Ca<sup>2+</sup>]<sub>i</sub> was seen between XL and CTR cells: the [Ca<sup>2+</sup>]<sub>i</sub> baselines in CTR and XL were 112.7 ±33.5 nM and 93.6±36.5 nM (n=19 experiments, 30-80 cells/experiment, p=0.114), respectively. Overall, the Ca<sup>2+</sup> signal in the Kv1.3-crosslinked cells was significantly higher than in control cells only when activated by the stimulus that induced the formation of an IS (with CD3/CD28 beads) (Fig. 4D). These findings indicate that the accumulation of Kv1.3 channels at the IS regulates the Ca<sup>2+</sup> response to antigen stimulation.

Further detailed analysis was done to determine whether Kv1.3 localization in the IS affects the kinetic of the Ca<sup>2+</sup> response. At the single cell level Jurkat T cells stimulated with beads display three characteristic Ca<sup>2+</sup> responses: oscillatory, sustained and transient (Fig. 5A). We found no difference in distribution of Ca<sup>2+</sup> responses of CTR and XL cells stimulated with beads (Fig. 5B). Similarly, there was no difference in the frequency of oscillations. The oscillation pattern in XL cells closely mirrored that of CTR cells with a median frequency response of 3.4 mHz. The detailed distribution for CTR and XL cells is shown in the frequency histogram in Fig. 5C. Overall, in Jurkat T cells blockade of Kv1.3 localization in the IS affects the magnitude, but not the kinetics, of [Ca<sup>2+</sup>]<sub>i</sub>.

## DISCUSSION

In this study we have shown that the recruitment of Kv1.3 to the IS occurs by lateral movement of surface channels along the plasma membrane. Furthermore, we found that Kv1.3 localization in the IS regulates the amplitude of the  $Ca^{2+}$  response that develops upon encounter with an APC. Thus, the dynamic recruitment of the plasma membrane-embedded Kv1.3 channels to the IS constitutes a part of the physiological function of the IS.

It has been shown that ion channels accumulate in the IS (8-11). Yet, the mechanisms and functional consequences of the channel targeting remain unknown. We have observed that antibody-based Kv1.3 crosslinking blocks the translocation of endogenous channels to the IS and the inhibition of protein synthesis did not influence the accumulation of channels to the IS (Figs 2 and 3). Furthermore, we found that Kv1.3 relocation into the IS does not involve a recycling process with endocytosis of membrane incorporated channels and their subsequent re-insertion in the plasma membrane. These observations strongly support the idea that the localization of native Kv1.3 channels in the IS occurs by lateral movement of surface channels along the plasma membrane. Other membrane proteins such as TCR and the integrin LFA-1 have been reported to move along the plasma membrane and accumulate at the IS via an actin-mediated process (28-30). Others suggested that a “diffusion trapping” process may be involved in the synapse formation (24,31,32). Molecular diffusion of proteins into the IS is initially random, although limited by various constraints such as the molecule size and association with other molecules. Once at the IS, diffusion is slowed, or even arrested, because new interactions occur with anchoring proteins. In neuronal and epithelial cells clustering and retention of ion channels within a particular plasma membrane domain involve, in part, the actin-cytoskeleton and scaffolding proteins that serve as a link between the channel and the cytoskeleton (33). In neurons the human homolog of the *Drosophila* discs large tumor suppressor protein (hDlg1), a PDZ protein of the membrane-associated guanylate kinase protein (MAGUK) family, acts as an anchor for voltage-gated  $K^+$  channels to allow specific subcellular localization (34). In immune cells, hDlg1 accumulates in the IS and coordinates actin polymerization and IS assembly (35,36). Immunoprecipitation studies in Jurkat T cells have shown that Kv1.3 exists in association with hDlg1 (37). Thus, it is possible that hDlg1 and the actin cytoskeleton may play a key role in Kv1.3 recruitment to the IS.

While the Kv1.3 crosslinking was useful to define the process by which Kv1.3 channels move into the IS, this procedure also provided us an experimental tool to study the functional relevance of Kv1.3 localization in the IS. We have compared the  $Ca^{2+}$  responses triggered upon formation of an IS (with CD3/CD28 beads) to the treatment with soluble CD3/CD28 antibodies. The latter intervention does not induce the formation of an IS. In agreement with a previous report, we observed different kinetics of the average  $Ca^{2+}$  response with two stimuli: a more sustained increase in  $[Ca^{2+}]_i$  with formation of the IS and transient changes in  $[Ca^{2+}]_i$  with soluble antibodies (17). This difference has been attributed to the redistribution of mitochondria to the IS which results in reduced local accumulation of  $Ca^{2+}$  and prolongation of  $Ca^{2+}$  entry through CRAC channels (17). Interestingly, we observed that prevention of Kv1.3 trafficking to the IS by crosslinking results in an exaggerated  $Ca^{2+}$  response only with CD3/CD28 beads. The Kv1.3 crosslinking neither affected the IS formation, as measured by F-actin and CD3 $\epsilon$  accumulation to the IS (Fig. 2), nor altered Kv1.3 activity (Fig. 1D). Moreover, soluble anti-CD3/CD28 antibody produced identical  $Ca^{2+}$  response in the crosslinked and control cells. Thus, the observed change in  $Ca^{2+}$  response is not due to altered channel activity, general disarrangement of the IS or non-functional  $Ca^{2+}$  reserves, but it correlates with the disrupted localization of Kv1.3 channels in the IS. However, we cannot exclude the possibility that Kv1.3 crosslinking might immobilize other factors important for the  $Ca^{2+}$  response. The crosslinking generated clusters/puncta of Kv1.3 proteins (Fig. 2 A and B). Although CD3 $\epsilon$  does not appear to be driven into this configuration, it is possible that other

membrane and signaling molecules tightly associated to the Kv1.3 proteins and clustered in these puncta might participate in the altered Ca<sup>2+</sup> response.

Overall these results provide compelling evidence that Kv1.3 accumulation in the IS is necessary for the development of a proper Ca<sup>2+</sup> response. Furthermore, they suggest that the IS may constitute a site for regulation of the Kv1.3 channel activity. Many signaling molecules recruited at the IS such as Lck, PKC $\theta$  and PKA have been shown to modulate the activity of Kv1.3 (38-44). Kv1.3 has multiple potential phosphorylation sites and it is likely that Kv1.3 localization in the IS is important to guarantee channel downregulation by signaling molecules accumulating at this site thus providing a feedback regulation of Ca<sup>2+</sup> signaling (38,39,45). Thus Kv1.3 inhibition at the IS would result in membrane depolarization that prevents, in normal conditions, the development of an exaggerated Ca<sup>2+</sup> response. Although blockade of Kv1.3 in the IS was not associated with altered Ca<sup>2+</sup> kinetics, defective permanence of the channel in the IS could affect the kinetics of the Ca<sup>2+</sup> response. If, for ex., the Kv1.3 channel enters in the IS, but it moves out prematurely, what would have normally being a transient Ca<sup>2+</sup> response could instead become more sustained because the channel downregulation is removed.

Overall altered Kv1.3 localization in the IS could have important patho-physiological consequences. Ca<sup>2+</sup> is a key regulator of the activity of transcription factors which control cytokine production and proliferation in T cells. It is well established that amplitude and duration of the Ca<sup>2+</sup> response determine the specificity of transcription factor activation and, consequently, the pattern of gene expression (46). We have reported that the movement of Kv1.3 is altered in T cells from patients with SLE and that a long-lasting localization in the IS, like the one that occurs in normal individuals, is instead short-lived in SLE (9). SLE T cells have been also reported to have more pronounced and sustained Ca<sup>2+</sup> signaling as well as increased NF-AT nuclear translocation than normal T cells (18,47). The data presented here indicate that defective Kv1.3 localization in the IS could indeed contribute to the Ca<sup>2+</sup> defect in these patients. Overall our studies raise the possibility that defects in ion channel trafficking to the IS could be involved in disease-associated abnormalities in Ca<sup>2+</sup> signaling.

## REFERENCES

1. Feske S. Calcium signalling in lymphocyte activation and disease. *Nat Rev Immunol* 2007;7:690–702. [PubMed: 17703229]
2. Feske S, Giltman J, Dolmetsch R, Staudt LM, Rao A. Gene regulation mediated by calcium signals in T lymphocytes. *Nature Immunology* 2001;2:316–324. [PubMed: 11276202]
3. Gallo EM, Cante-Barrett K, Crabtree GR. Lymphocyte calcium signaling from membrane to nucleus. *Nat Immunol* 2006;7:25–32. [PubMed: 16357855]
4. Lewis RS. Calcium signaling mechanisms in T lymphocytes. *Annu. Rev. Immunol* 2001;19:497–521. [PubMed: 11244045]
5. Lewis RS. The molecular choreography of a store-operated calcium channel. *Nature* 2007;446:284–287. [PubMed: 17361175]
6. Koo GC, Blake JT, Talento A, Nguyen M, Lin S, Sirotina A, Shah K, Mulvany K, Hora D Jr, Cunningham P, Wunderler DL, McManus OB, Slaughter R, Bugianesi R, Felix J, Garcia M, Williamson J, Kaczowski G, Sigal NH, Springer MS, Feeney W. Blockade of the voltage-gated potassium channel Kv1.3 inhibits immune responses in vivo. *J Immunol* 1997;158:5120–5128. [PubMed: 9164927]
7. Leonard RJ, Garcia ML, Slaughter RS, Reuben JP. Selective blockers of voltage-gated K<sup>+</sup> channels depolarize human T lymphocytes: mechanism of the antiproliferative effect of charybdotoxin. *Proc Natl Acad Sci U S A* 1992;89:10094–10098. [PubMed: 1279670]
8. Panyi G, Vamosi G, Bacso Z, Bagdany M, Bodnar A, Varga Z, Gaspar R, Matyus L, Damjanovich S. Kv1.3 potassium channels are localized in the immunological synapse formed between cytotoxic and target cells. *Proc Natl Acad Sci U S A* 2004;101:1285–1290. [PubMed: 14745040]



9. Nicolaou SA, Szigligeti P, Neumeier L, Lee SM, Duncan HJ, Kant SK, Mongey AB, Filipovich AH, Conforti L. Altered Dynamics of Kv1.3 Channel Compartmentalization in the Immunological Synapse in Systemic Lupus Erythematosus. *J Immunol* 2007;179:346–356. [PubMed: 17579055]
10. Nicolaou SA, Neumeier L, Peng Y, Devor DC, Conforti L. The Ca<sup>2+</sup>-activated K<sup>+</sup> channel KCa3.1 compartmentalizes in the immunological synapse of human T lymphocytes. *Am J Physiol Cell Physiol* 2007;292:C1431–1439. [PubMed: 17151145]
11. Lioudyno MI, Kozak JA, Penna A, Safrina O, Zhang SL, Sen D, Roos J, Stauderman KA, Cahalan MD. Orail 1 and STIM1 move to the immunological synapse and are up-regulated during T cell activation. *Proceedings of the National Academy of Sciences* 2008;105:2011–2016.
12. Cemerski S, Shaw A. Immune synapses in T-cell activation. *Current Opinion in Immunology* 2006;18:298–304. [PubMed: 16603343]
13. Lin J, Miller MJ, Shaw AS. The c-SMAC: sorting it all out (or in). *J Cell Biol* 2005;170:177–182. [PubMed: 16009722]
14. Varma R, Campi G, Yokosuka T, Saito T, Dustin ML. T cell receptor-proximal signals are sustained in peripheral microclusters and terminated in the central supramolecular activation cluster. *Immunity* 2006;25:117–127. [PubMed: 16860761]
15. Mossman KD, Campi G, Groves JT, Dustin ML. Altered TCR Signaling from Geometrically Repatterned Immunological Synapses. *Science* 2005;310:1191–1193. [PubMed: 16293763]
16. Groves JT. Spatial mutation of the T cell immunological synapse. *Curr Opin Chem Biol* 2006;10:544–550. [PubMed: 17070724]
17. Quintana A, Schwindling C, Wenning AS, Becherer U, Rettig J, Schwarz EC, Hoth M. T cell activation requires mitochondrial translocation to the immunological synapse. *Proc Natl Acad Sci U S A*. 2007
18. Kyttaris VC, Wang Y, Juang YT, Weinstein A, Tsokos GC. Increased levels of NF-ATc2 differentially regulate CD154 and IL-2 genes in T cells from patients with systemic lupus erythematosus. *J Immunol* 2007;178:1960–1966. [PubMed: 17237447]
19. Conforti L, Petrovic M, Mohammad D, Lee S, Ma Q, Barone S, Filipovich AH. Hypoxia regulates expression and activity of kv1.3 channels in T lymphocytes: a possible role in T cell proliferation. *J Immunol* 2003;170:695–702. [PubMed: 12517930]
20. Robbins JR, Lee SM, Filipovich AH, Szigligeti P, Neumeier L, Petrovic M, Conforti L. Hypoxia modulates early events in T cell receptor-mediated activation in human T lymphocytes via Kv1.3 channels. *J Physiol* 2005;564:131–143. [PubMed: 15677684]
21. Fanger CM, Neben AL, Cahalan MD. Differential Ca<sup>2+</sup> influx, KCa channel activity, and Ca<sup>2+</sup> clearance distinguish Th1 and Th2 lymphocytes. *J Immunol* 2000;164:1153–1160. [PubMed: 10640725]
22. Dolmetsch RE, Lewis RS. Signaling between intracellular Ca<sup>2+</sup> stores and depletion-activated Ca<sup>2+</sup> channels generates [Ca<sup>2+</sup>]<sub>i</sub> oscillations in T lymphocytes. *J Gen Physiol* 1994;103:365–388. [PubMed: 8195779]
23. Pongs O, Leicher T, Berger M, Roeper J, Bähring R, Wray D, Giese KP, Silva AJ, Storm JF. Functional and molecular aspects of voltage-gated K<sup>+</sup> channel beta subunits. *Ann N Y Acad Sci* 1999;868:344–355. [PubMed: 10414304]
24. Favier B, Burroughs NJ, Wedderburn L, Valitutti S. TCR dynamics on the surface of living T cells. *Int. Immunol* 2001;13:1525–1532. [PubMed: 11717193]
25. Jugloff DG, Khanna R, Schlichter LC, Jones OT. Internalization of the Kv1.4 potassium channel is suppressed by clustering interactions with PSD-95. *J Biol Chem* 2000;275:1357–1364. [PubMed: 10625685]
26. Choi WS, Khurana A, Mathur R, Viswanathan V, Steele DF, Fedida D. Kv1.5 surface expression is modulated by retrograde trafficking of newly endocytosed channels by the dynein motor. *Circ Res* 2005;97:363–371. [PubMed: 16051887]
27. Quintana A, Griesemer D, Schwarz EC, Hoth M. Calcium-dependent activation of T-lymphocytes. *Pflügers Archiv European Journal of Physiology* 2005;450:1–12.
28. Kaizuka Y, Douglass AD, Varma R, Dustin ML, Vale RD. Mechanisms for segregating T cell receptor and adhesion molecules during immunological synapse formation in Jurkat T cells. *Proc Natl Acad Sci U S A* 2007;104:20296–20301. [PubMed: 18077330]

29. Ralston KJ, Hird SL, Zhang X, Scott JL, Jin B, Thorne RF, Berndt MC, Boyd AW, Burns GF. The LFA-1-associated Molecule PTA-1 (CD226) on T Cells Forms a Dynamic Molecular Complex with Protein 4.1G and Human Discs Large. *J. Biol. Chem* 2004;279:33816–33828. [PubMed: 15138281]
30. Dustin ML. T-cell activation through immunological synapses and kinapses. *Immunological Reviews* 2008;221:77–89. [PubMed: 18275476]
31. Davis SJ, van der Merwe PA. The kinetic-segregation model: TCR triggering and beyond. *Nat Immunol* 2006;7:803–809. [PubMed: 16855606]
32. Douglass AD, Vale RD. Single-molecule microscopy reveals plasma membrane microdomains created by protein-protein networks that exclude or trap signaling molecules in T cells. *Cell* 2005;121:937–950. [PubMed: 15960980]
33. Mazzochi C, Benos DJ, Smith PR. Interaction of epithelial ion channels with the actin-based cytoskeleton. *Am J Physiol Renal Physiol* 2006;291:F1113–1122. [PubMed: 16926444]
34. Kim E, Niethammer M, Rothschild A, Jan YN, Sheng M. Clustering of Shaker-type K<sup>+</sup> channels by interaction with a family of membrane-associated guanylate kinases. *Nature* 1995;378:85–88. [PubMed: 7477295]
35. Xavier R, Rabizadeh S, Ishiguro K, Andre N, Ortiz JB, Wachtel H, Morris DG, Lopez-Illasaca M, Shaw AC, Swat W, Seed B. Discs large (Dlg1) complexes in lymphocyte activation. *J Cell Biol* 2004;166:173–178. [PubMed: 15263016]
36. Round JL, Tomassian T, Zhang M, Patel V, Schoenberger SP, Miceli MC. Dlg1 coordinates actin polymerization, synaptic T cell receptor and lipid raft aggregation, and effector function in T cells. *J Exp Med* 2005;201:419–430. [PubMed: 15699074]
37. Hanada T, Lin L, Chandy KG, Oh SS, Chishti AH. Human Homologue of the Drosophila Discs Large Tumor Suppressor Binds to p56lck Tyrosine Kinase and Shaker Type Kv1.3 Potassium Channel in T Lymphocytes. *J. Biol. Chem* 1997;272:26899–26904. [PubMed: 9341123]
38. Cai YC, Douglass J. In vivo and in vitro phosphorylation of the T lymphocyte type n (Kv1.3) potassium channel. *J Biol Chem* 1993;268:23720–23727. [PubMed: 8226897]
39. Holmes TC, Fadool DA, Levitan IB. Tyrosine phosphorylation of the Kv1.3 potassium channel. *J Neurosci* 1996;16:1581–1590. [PubMed: 8774427]
40. Payet MD, Dupuis G. Dual regulation of the n type K<sup>+</sup> channel in Jurkat T lymphocytes by protein kinases A and C. *J Biol Chem* 1992;267:18270–18273. [PubMed: 1326519]
41. Martel J, Dupuis G, Deschenes P, Payet MD. The sensitivity of the human Kv1.3 (hKv1.3) lymphocyte K<sup>+</sup> channel to regulation by PKA and PKC is partially lost in HEK 293 host cells. *J Membr Biol* 1998;161:183–196. [PubMed: 9435274]
42. Szigligeti P, Neumeier L, Duke E, Chougnet C, Takimoto K, Lee SM, Filipovich AH, Conforti L. Signalling during hypoxia in human T lymphocytes - critical role of the src protein tyrosine kinase p56Lck in the O<sub>2</sub> sensitivity of Kv1.3 channels. *J Physiol* 2006;573:357–370. [PubMed: 16600997]
43. Fadool DA. Tyrosine phosphorylation downregulates a potassium current in rat olfactory bulb neurons and a cloned Kv1.3 channel. *Ann N Y Acad Sci* 1998;855:529–532. [PubMed: 9929647]
44. Fadool DA, Holmes TC, Berman K, Dagan D, Levitan IB. Tyrosine phosphorylation modulates current amplitude and kinetics of a neuronal voltage-gated potassium channel. *J Neurophysiol* 1997;78:1563–1573. [PubMed: 9310443]
45. Chung I, Schlichter LC. Native Kv1.3 channels are upregulated by protein kinase C. *J Membr Biol* 1997;156:73–85. [PubMed: 9070466]
46. Scharenberg AM, Humphries LA, Rawlings DJ. Calcium signalling and cell-fate choice in B cells. *Nat Rev Immunol* 2007;7:778–789. [PubMed: 17853903]
47. Krishnan S, Farber DL, Tsokos GC. T Cell Rewiring in Differentiation and Disease. *J Immunol* 2003;171:3325–3331. [PubMed: 14500623]

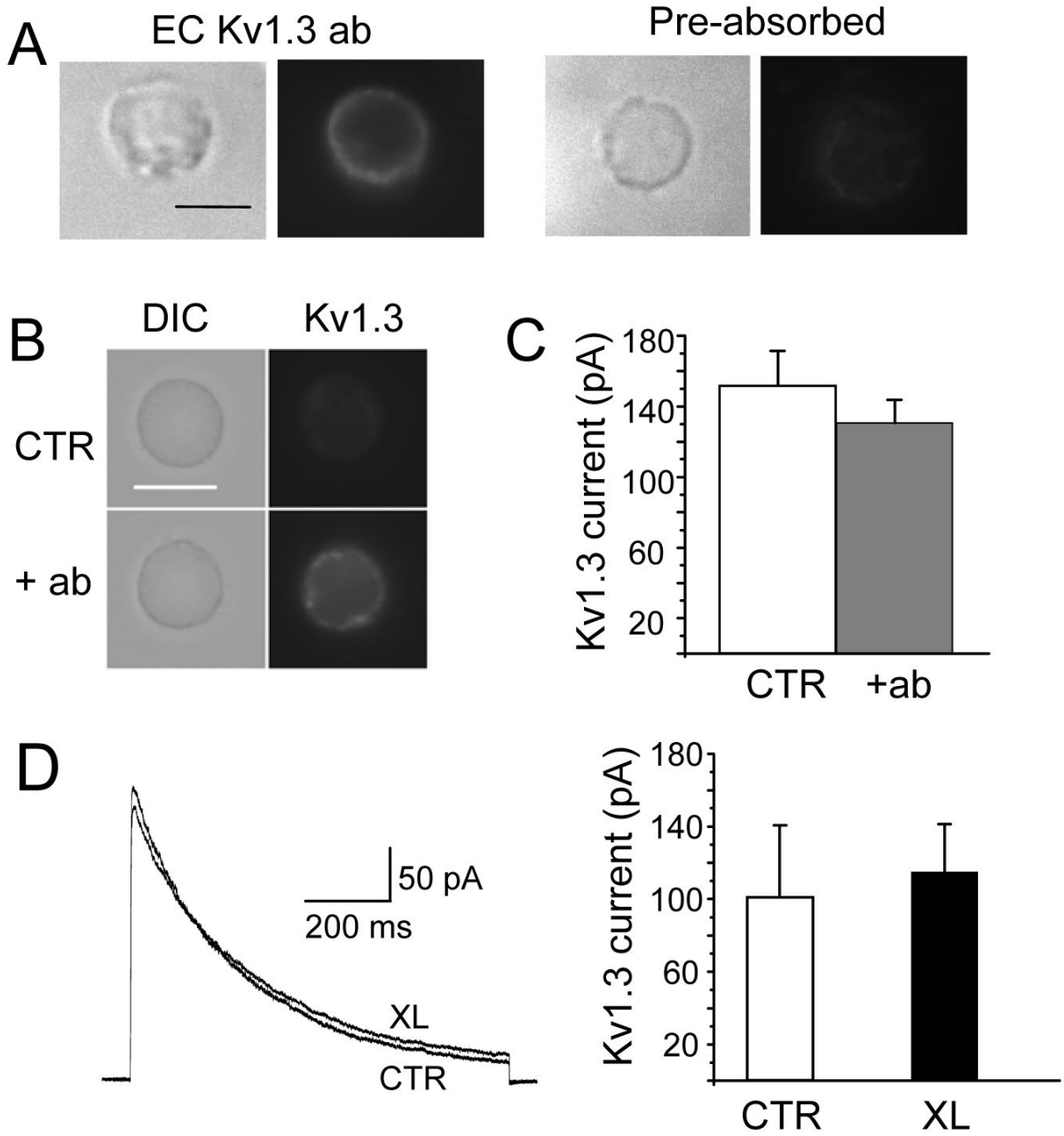


**Figure 1.** Specificity and lack of functional effects of extracellular anti-Kv1.3 antibody (EC Kv1.3 ab). A. Human T cells were fixed and stained with EC-Kv1.3 antibody (left) or anti-Kv1.3 antibody pre-adsorbed to the antigen (right). The corresponding DIC and fluorescence micrographs for each set are shown. B-C. Jurkat T cells were incubated with EC-Kv 1.3 antibody at 1:1 and 100:1 ratio of antibody:Kv1.3  $\alpha$  subunit for 30 min at 37°C. After this time, cells were either patched or fixed and stained with secondary antibodies. The DIC and fluorescent images for Kv1.3 are shown for controls (no antibody) and cells treated with a 1:1 antibody:Kv1.3  $\alpha$  in panel B. For electrophysiological experiments, Kv1.3 currents were elicited by depolarizing voltages to +50 mV (-80 mV HP). The average Kv1.3 current for control (CTR, n=15) and T cell treated with a 100:1 antibody:Kv1.3  $\alpha$  (n=16) are reported in panel C. There was no difference between the two groups (p=0.18). The capacitance measured was similar in the two

groups ( $8.6 \pm 0.4$  pF for control and  $8.1 \pm 0.5$  pF for antibody-treated cells,  $p=0.25$ ). D. Kv1.3 crosslinking does not affect the activity of Kv1.3. Kv1.3 currents were recorded in Jurkat T cells after Kv1.3 crosslinking (XL) and compared to control (CTR, no antibody) cells. Representative traces in CTR and XL cells are shown in the left panel. Currents were elicited by depolarizing voltage steps to +50 mV (-80 mV HP). The average current amplitudes for CTR (n=6) and XL (n=8) are reported in the right panel. There was no difference in capacitance among these groups ( $3.8 \pm 0.3$  pF for CTR and  $3.6 \pm 0.3$  pF for XL).

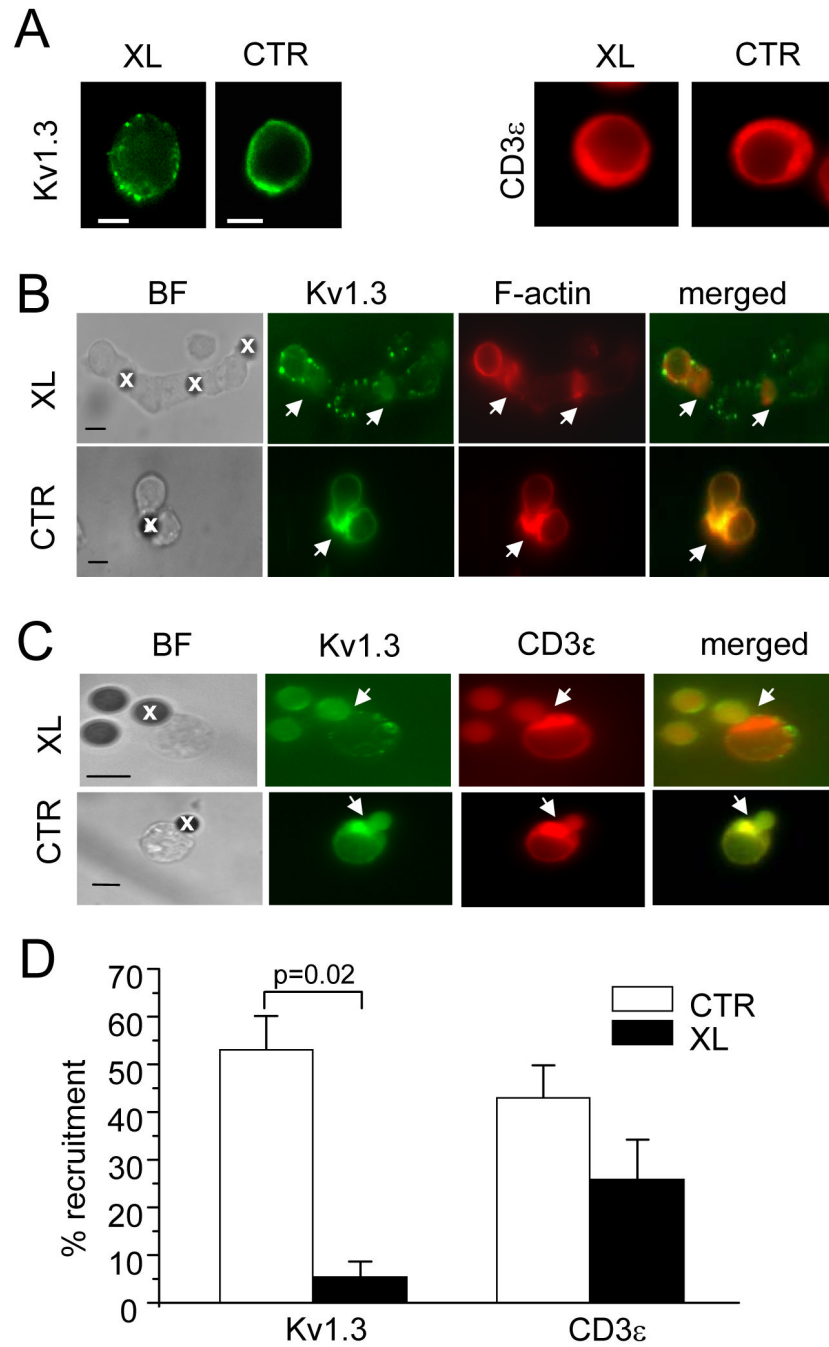


**Figure 2.** Kv1.3 redistribution in the immunological synapse occurs by lateral movement of membrane channels. **A.** Kv1.3 (left) and CD3ε (right) distribution in resting T cells (not exposed to CD3/CD28 beads) in Kv1.3 crosslinking (XL) and control (CTR) cells. **B.** Kv1.3 distribution to the IS. Jurkat cells were treated with anti-Kv1.3 antibody only (bottom, CTR) or anti-Kv1.3 antibody and crosslinked (top). Cells were then exposed to CD3/CD28 beads for 15 min and fixed. Kv1.3 was identified with Alexa Fluor 488 secondary antibody (green), F-actin by fluorescently labeled phalloidin (red). The merged images are shown in the right panels. Beads are marked by x in the brightfield (BF) images. The arrows indicate the IS. **C.** Differential distribution of Kv1.3 and CD3ε. Cell were pre-treated with Kv1.3 antibody as described in B

and the distribution of Kv1.3 (green) and CD3 $\epsilon$  (red) in the IS assessed after exposure to CD3/CD28 beads. Scale bars, 5  $\mu$ m. D. Average Kv1.3 and CD3 $\epsilon$  recruitment in the IS in CTR and XL cells. The % of cells that display either Kv1.3 or CD3 $\epsilon$  accumulation in the IS is reported as % of cells with Kv1.3/CD3 $\epsilon$  polarized at the site of contact relative to the number of cells that made contact with beads. Kv1.3 and CD3 $\epsilon$  recruitment was determined in parallel on the same set of photographs. The data shown are the average responses collected from 3 separate experiments with a total of 77-102 T cell-bead conjugates/experiment.

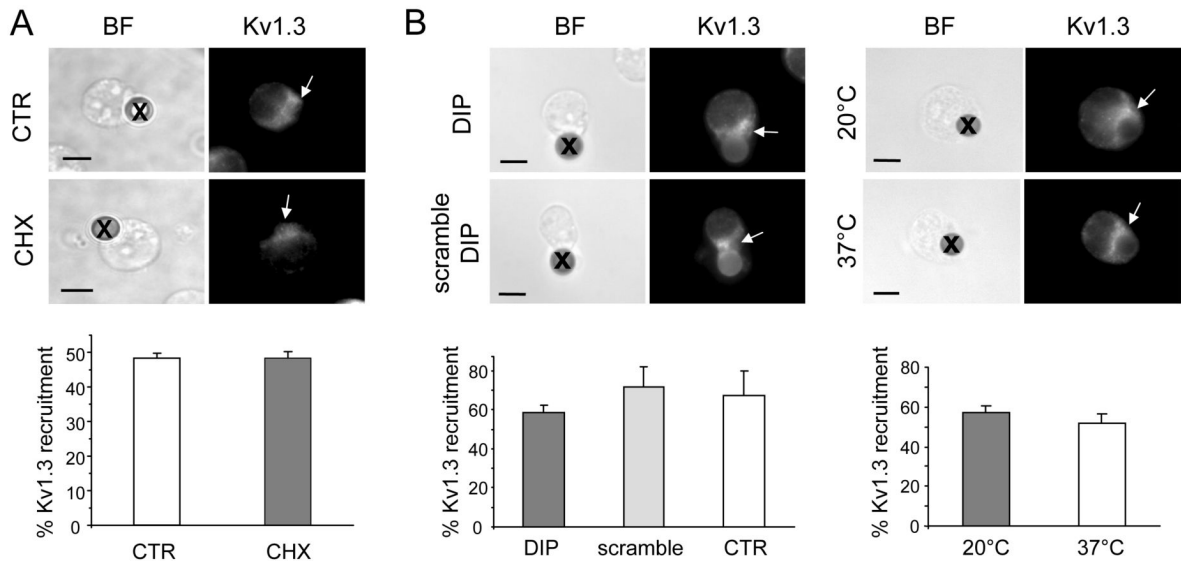


**Figure 3.**

Mature Kv1.3 channels move to the immunological synapse by lateral diffusion along the plane of the plasma membrane. A. Newly synthesized Kv1.3 channels are not recruited in the immune synapse. T cells were treated with cycloheximide (CHX, 10 uM) and Kv1.3 polarization in the IS compared with that of control cells (CTR, no CHX). Cells were maintained with and without CHX overnight, then exposed to CD3/CD28 beads for 15 min and fixed. Top: photomicrographs of T/bead conjugates in presence (CHX) or absence (CTR) of CHX. Kv1.3 was labeled with EC-Kv1.3 antibody and identified with Alexa Fluor 488 secondary antibody (right panels). Beads are marked by x in the BF images and the IS by arrows in the fluorescent images. Bottom: Average Kv1.3 recruitment in the IS in CTR and CHX-treated cells. The % of cells that display Kv1.3 accumulation in the IS is calculated as described in figure 2D. The data shown are the average responses collected from 3 separate experiments with a total of 49-89 T cell-bead conjugates/experiment. B. Endocytosis and exocytosis are not involved in Kv1.3 movement to the immune synapse. Left: Comparisons were made between cells treated overnight with DIP (which inhibits endocytosis) and its inactive control (scramble DIP) at 50 uM. We measured the percentage of Kv1.3 recruitment in the IS after 15 min exposure to beads as described in A. Right: Comparisons were made between cells maintained at 20°C (a condition that inhibits exocytosis) for 2 hr and throughout the experiment, and cells maintained at 37°C. The percentage Kv1.3 recruitment into the IS was determined after 15 min treatment with CD3/CD28 beads. Top panels show Kv1.3 recruitment in the IS in the different experimental conditions. The corresponding average data are shown below in the left panel for DIP-, scramble DIP-treated cells and control (CTR, non treated) cells and in the right panel for 20°C and 37°C (n=3 separate experiments; 50 to 100 conjugates/experiment).

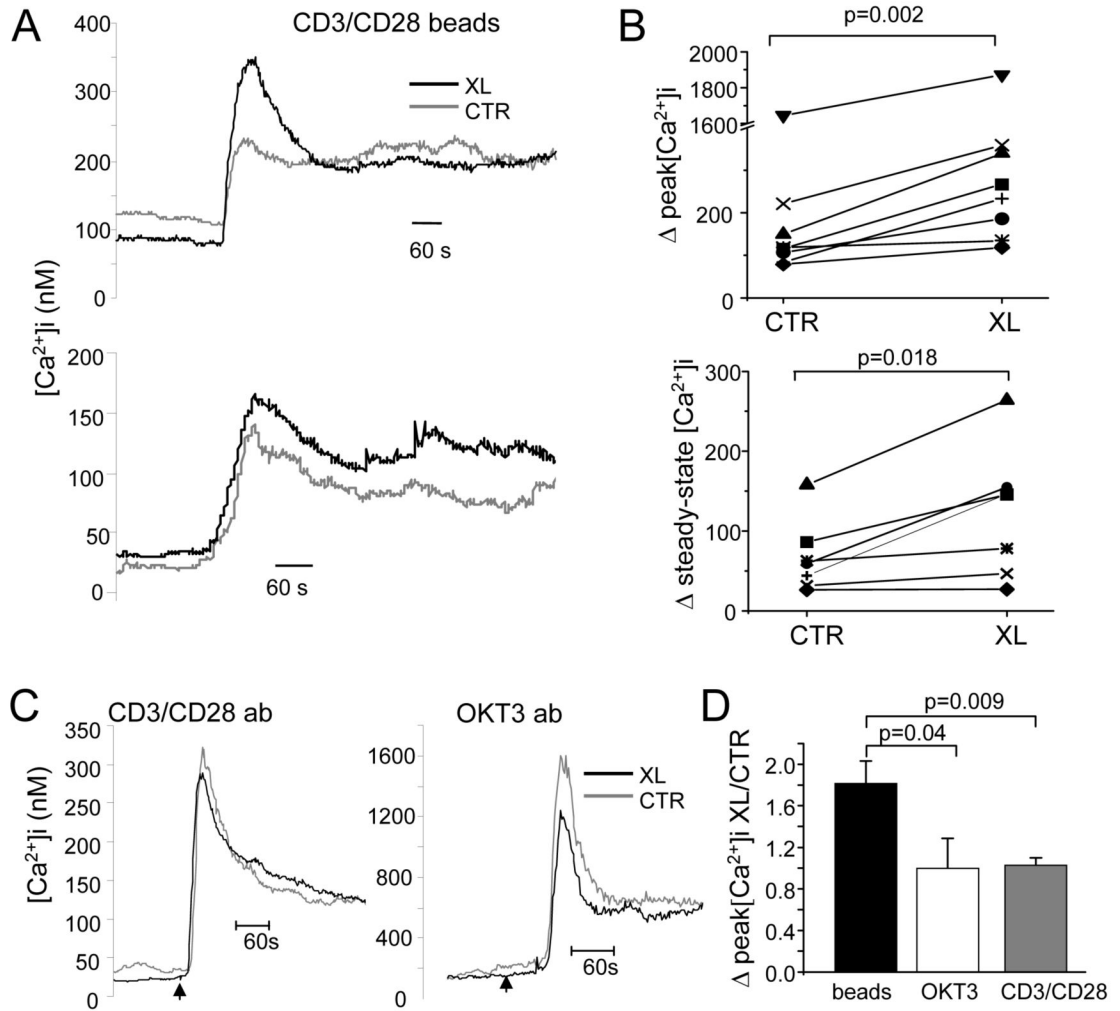


**Figure 4.**

Blockade of Kv1.3 accumulation in the immune synapse alters Ca<sup>2+</sup> signaling. A. Ca<sup>2+</sup> response was measured by Fura-2 and elicited by CD3/CD28 beads in control (CTR) and Kv1.3 crosslinked (XL) cells. The average increase in [Ca<sup>2+</sup>]<sub>i</sub> of responding cells is reported for two representative experiments (average of 55-78 cells). B. Summary of the increase in peak (top) and steady-state (5 min from Ca<sup>2+</sup> onset; bottom) [Ca<sup>2+</sup>]<sub>i</sub> induced by CD3/CD28 beads. Changes in [Ca<sup>2+</sup>]<sub>i</sub> were taken from measuring the values of peak and steady-state [Ca<sup>2+</sup>]<sub>i</sub> and expressing them as changes in [Ca<sup>2+</sup>]<sub>i</sub> from baseline levels (Δ[Ca<sup>2+</sup>]<sub>i</sub>). Each value is the average of 35-78 cells/experiment. C. Representative average Ca<sup>2+</sup> responses elicited in CTR and XL cells with a mixture of soluble CD3 and CD28 antibodies (CD3/CD28 ab, 5ug/ml each) and soluble CD3 antibody (OKT3; 5 ug/ml). Each trace is an average of 63-75 cells. D. Comparison of the effect of XL on the Ca<sup>2+</sup> response elicited by CD3/CD28 beads (beads), OKT3 and CD3/CD28 ab. The ratio of the increase in peak [Ca<sup>2+</sup>]<sub>i</sub> in XL and CTR cells is reported for cells stimulated with beads (n=8), OKT3 (n=5) and CD3/CD28 ab (n=6).



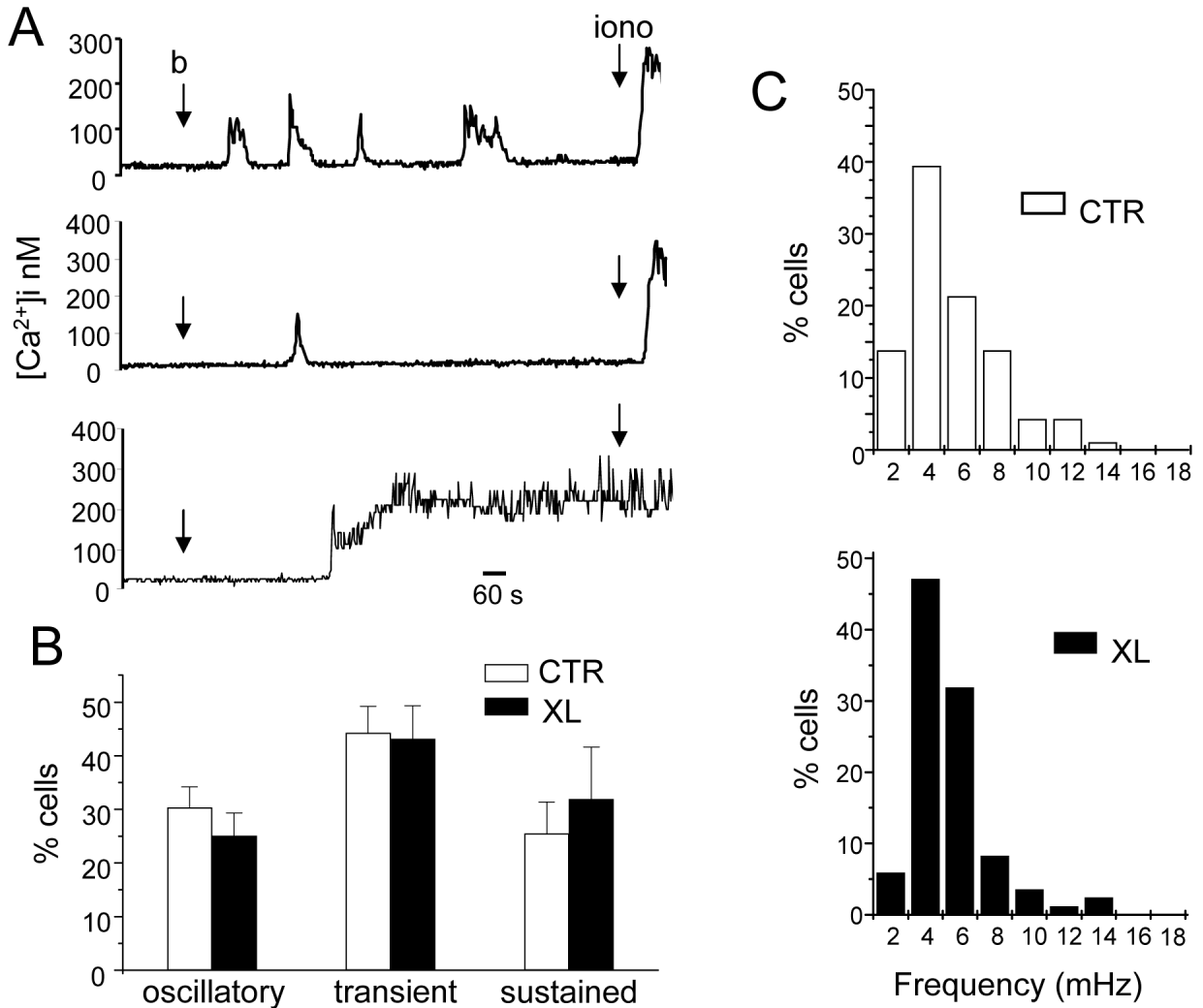


**Figure 5.** Blockade of Kv1.3 movement to the immune synapse does not affect the distribution of  $Ca^{2+}$  responses and the frequency of oscillations. A. Representative  $Ca^{2+}$  responses induced by CD3/CD28 beads in individual cells. The points of introduction of the beads (b) and ionomycin (iono, 1-2  $\mu$ M) into the bath are indicated by arrows. Contact with beads triggered various responses including oscillatory (top), transient (middle) and sustained (bottom)  $Ca^{2+}$  responses. B. Average  $[Ca^{2+}]_i$  response distribution in CTR and XL cells. Number of cells displaying a transient, sustained or oscillatory response are reported as normalized for the total number of T cells that show an increase in  $[Ca^{2+}]_i$  upon exposure to beads. The data are the average of 8 experiments (same experiments shown in Fig. 4). C. Distribution of oscillation frequencies. The distribution of oscillation frequencies for CTR and XL cells are shown in the top and bottom panels, respectively (n=8 experiments and a total of 94 cells for CTR and 85 for XL). Results are presented as percentage of cells, within the oscillating population, displaying a particular frequency.